Insight into the spin state at the surface of $LaCoO_3$ revealed by photoemission electron microscopy

A. A. Yaroslavtsev,[1,2,3] M. Izquierdo,[1,2] R. Carley,[1] M. E. Dávila,[4] A. A. Ünal,[5] F. Kronast,[5] A. Lichtenstein,[1,2,6] A. Scherz,[1] and S. L. Molodtsov[1,7,8]

[1]*European XFEL GmbH, Albert-Einstein-Ring 19, 22761 Hamburg, Germany*

[2]*Institut für Theoretische Physik, Universität Hamburg, Jungiusstraße 9, 20355 Hamburg, Germany*

[3]*National Research Nuclear University "MEPhI", Kashirskoe Shosse 31, 115409 Moscow, Russia*

[4]*Instituto de Ciencia de Materiales de Madrid-ICMM-CSIC, C/Sor Juana Inés de la Cruz, 3 Cantoblanco, 28049 Madrid, Spain*

[5]*Helmholtz-Zentrum Berlin für Materialien und Energie GmbH, BESSY II, Albert-Einstein-Straße 15, 12489 Berlin, Germany*

[6]*Ural Federal University, 620990 Yekaterinburg, Russia*

[7]*Institute of Experimental Physics, Technische Universität Bergakademie Freiberg, 09599 Freiberg, Germany*

[8]*ITMO University, Kronverkskiy Prospect 49, 197101 St. Petersburg, Russia*

(Received 13 January 2016; revised manuscript received 9 March 2016; published 20 April 2016)

The evolution of the spin transition in $LaCoO_3$ has been investigated with photoemission electron microscopy (PEEM) as a function of temperature. The investigated temperature range spanned from a predominantly low spin configuration (125 K) to the proposed percolation limit for metallization (413 K). The data show that the spin configuration exhibits an inhomogeneous spatial distribution that is very sensitive to the surface preparation method. In the region of the semiconductor-to-metal transition (300 to 450 K), the spatial contrast is continuously reduced, indicating a smooth transition without domain percolation. These observations support a new interpretation of the temperature evolution of the system that is in agreement with current theoretical understanding of the spin transition.

DOI: 10.1103/PhysRevB.93.155137

I. INTRODUCTION

At a time when environmental preservation and optimization of natural resources are of primary importance, enormous efforts are concentrated in finding materials allowing efficient energy production [1–5]. They are meant to substitute costly precious catalytic metals such as Pt. In addition to their high cost, precious metal catalysts can lead to soil contamination when released into the environment. In this context, $LaCoO_3$ (LCO) has received much attention due to its potential applications in energy related processes taking place at high temperature. These include catalytic oxidation of hydrocarbons [2], volatile organic contaminants (VOCs) [3], and CO and lean NO_x trapping [1,5]. Higher catalytic activity and thermal stability have been observed compared to Pt-based materials. These results could lead, for example, to a new generation of devices for use in diesel engines [5]. The application of these materials in practical devices may be more rapidly realized due to the development of new polymer assisted deposition methods [6]. Upon an appropriate selection of the substrate, the strain in the deposited thin films can be controlled to enhance the catalytic activity [7].

Possible applications of LCO are derived from its physical properties. These are characterized by a diamagnetic-to-paramagnetic spin transition at ≈100 K, and a broad semiconductor-to-metal (SM) transition between 350 and 650 K. Changes in the structure, phonon spectrum, and transport properties are observed across these transitions [8–13]. The nature of the spin transition has been discussed largely in terms of competition between high spin (HS) and intermediate spin (IS) configurations [14–21]. However, the most recent experiments and theoretical calculations favor the LS-to-HS transition [17–21] [Fig. 1(a)]. The detailed description of the transition is made more complicated by the presence of charge imbalance induced by correlations. The two Co ions in the unit cell have asymmetric d^5 and d^7 charge contributions. The relative population of these states changes with temperature, maintaining on average a d^6 electronic configuration of Co with a constant valence of oxygen (−2) and lanthanum (+3) [21]. On the other hand the SM transition, which extends over a very large temperature range, has been much less studied. It has been assumed up to now that the SM transition involves a continuous change of the spin state and the coexistence of semiconducting and metallic domains.

Nevertheless, several questions remain open regarding the details of the metallization process. In the 1970s Goodenough *et al.* proposed a mechanism based on the percolation of domains [10,11]. To the best of our knowledge, however, such a scenario has not yet been experimentally confirmed. Clarifying the role of the percolation mechanism is of critical importance to optimize the catalytic applications of this compound. If semiconducting and metallic domains coexist then the catalytic activity will depend on the particular electronic state at different positions in the sample for temperatures below the full metallization regime, i.e., <650 K. If the metallization does not occur via a percolation process then the catalytic activity would depend more on other parameters such as the modification of the band structure with temperature. It has been indeed shown that above 350 K the system exhibits both high electronic and high ionic conductivities that are relevant for the catalytic activity [1–5]. Strain and oxygen vacancies induced by doping also increase the catalytic activity [7,22]. The fact that substrate strain has also allowed one to realize states with atomic resolved spin order [23] supports the existence of a direct link between the spin state and the catalytic applications.

Although the LCO catalytic activity has been extensively studied for potential application at high temperatures, the electronic properties have been less thoroughly investigated. The temperature-dependent studies of the electronic properties of LCO have been only reported on length scales larger than several micrometers [14,17,24–28].

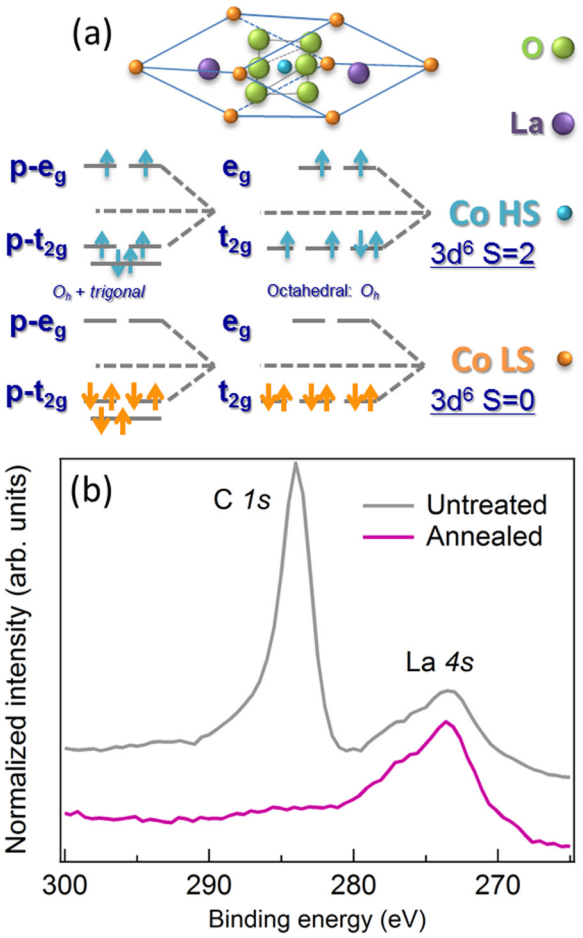

FIG. 1. (a) Rhombohedral crystal lattice and orbital filling in the single-electron picture for the octahedral crystal field (bottom left) and the real trigonal distorted one (bottom right). The weak trigonal distortion allows treating the Co orbitals as pseudo-t_{2g}(p-t_{2g}) and pseudo-e_g(p-e_g). (b) Photoemission spectra measured at 1000 eV for the untreated sample (grey) and after two-cycles of annealing in oxygen (purple). No traces of carbon contamination can be observed after annealing.

In this paper, we report photoemission electron microscopy (PEEM) investigations that reveal the electronic and spin properties of LCO as a function of temperature with nanometer spatial resolution. Over a temperature range of 125 to 413 K, which includes the first steps of metallization, the results show an inhomogeneous spatial distribution of the spin configuration that is more pronounced at low temperatures. Upon increasing temperature the spatial contrast decreases. The high intensity domains ascribed to higher metallicity show no correlation with temperature. This does not favor the percolation model for the metallization process in LCO [10,11]. The results are more in agreement with the current theoretical understanding of the spin evolution with temperature [20,21,29].

II. EXPERIMENTAL DETAILS

The experiments were performed at the spin-resolved photoemission electron microscope (SPEEM) branch of the UE49-PGMa beamline at the BESSY II storage ring at Helmholz-Zentrum-Berlin. The undulator source produces soft x rays with variable polarization in the spectral range from 80 to 1800 eV. The optical system monochromatizes the incoming beam with a resolving power $E/\Delta E = 10\,000$ at 700 eV and focuses the x-ray beam down to $20 \times 30\ \mu m^2$ (vertical $\times$ horizontal). The photon flux in the focus is of the order of 2×10^{12} photons/s between the O K and the La M edges for 100 mA ring current. The PEEM images were recorded with a commercial ELMITEC microscope giving 25 nm spatial resolution when working with a 3 μm field of view. The sample manipulator is equipped with a combined cryostat-heating stage that allows the temperature to be varied between 45 and 600 K.[1] The sample depth of the PEEM varied between $\simeq$27 Å at 500 eV and 45 Å at 1000 eV. These values correspond to 3λ, where λ is the electron scape depth at the given photon energy.

LCO single crystals of $4 \times 4 \times 0.5\,mm^3$ with a (001) surface termination from SurfaceNet GmbH were used in the experiments. They were cleaned by annealing cycles of 1 hour in an oxygen atmosphere at 8×10^{-6} mbar. This preparation technique results in clean samples [24]. Figure 1(b) shows photoemission spectra measured at 1000 eV for the untreated sample and after oxygen annealing. No traces of carbon contamination were observed at the surface after two annealing cycles. The absence of a low energy electron diffraction (LEED) apparatus in the experimental setup prevented measurement of the surface reconstruction. However, theoretical work suggests reconstruction should occur to avoid dipolar surfaces [30,31].

Two consecutive series of measurements were performed as a function of the temperature in the range from 125 to 413 K. This temperature is sufficient to probe the existence of a percolation onset, provided this is the mechanism driving the metallization of the system. The first series was carried out directly after surface preparation with a spatial resolution of $\approx$125 nm. Since the analysis of the data (see below) suggested that the resolution was not sufficient to resolve the spatial extend of the modifications induced upon heating, a second series of measurements, named series 2 in the following, was carried out. Directly after the series 1 measurements, the sample was cooled down without any additional treatment and the measurements repeated with a spatial resolution of 25 nm. The improved resolution allowed us to observe sharp features on the images that have allowed understanding of the development of metallization with temperature.

III. RESULTS

In the first series of measurements the PEEM scans were taken at the O K, Co L, and La M edges with a field of view (FOV) of 50 μm (spatial resolution $\approx$125 nm) as a function of temperature. In Fig. 2, left panel top row, $7 \times 7\ \mu m^2$ fragments of the images taken at the O K edge ($\sim$529 eV) for different temperatures are shown after normalization to the incoming photon flux. The images at the Co $L_{3,2}$ and La $M_{5,4}$ absorption edges (not shown) are similar, indicating strong spatial correlation. One can distinguish dark

[1]At the time the experiments were carried out the low temperature limit was 100 K and only 413 K were accessible due to a grounding problem of the current source used to increase the current.

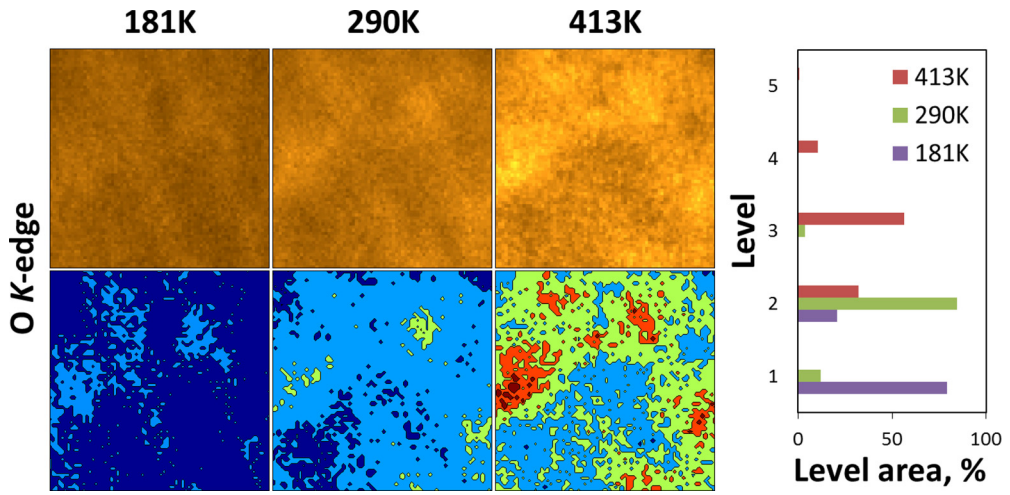

FIG. 2. (Left panel) Temperature evolution of resonant PEEM images (7×7 μm^2 fragments) at the O K edge (~529 eV): raw images (top panel) and images after binning into five levels. We can see clear contrast modifications with temperature. (Right panel) Population of brightness levels for PEEM images at the O K edge for the data shown on the left. A clear shift in the populations can be seen with temperature, indicating that the surface is more homogeneous and more insulating at lower temperature.

(low photoemission intensity) and bright (high photoemission intensity) regions without well defined contours. This suggests that the spatial changes take place within a scale smaller than the resolution (<125 nm). We can also observe that the images at low temperature are overall darker, and exhibit much less contrast than those measured at high temperature.

In order to extract quantitative information from the images, they were binned into levels with intensities varying between the minimum and maximum values of the image at 413 K (Fig. 2, left panel bottom row). At this temperature, for which the contrast is maximum, five levels were obtained. At 290 and 181 K only three and two levels could be obtained, respectively, due to the reduced contrast observed at lower temperatures. The relative population of the different levels is shown in Fig. 2 (right panel) as a function of the temperature. We can see that at 181 K 75% of the analyzed sample is level 1 (dark). As the temperature is increased to room temperature the largest population, >80%, goes to level 2. Finally at 413 K the sample is less homogenous with a content of level 3 of only 50%, the remaining being mainly levels 2 and 4.

To understand the temperature evolution of the sample, x-ray absorption spectra (XAS) were analyzed for the most highly populated level at each temperature: level 1 at 181 K, level 2 at 290 K, and level 3 at 413 K. A similar treatment to that described for the O K-edge data was carried out on the Co L_3-edge data and shows similar level population. The XAS spectra as a function of the temperature for both edges are displayed in Fig. 3 after normalization to the maximum intensity in each spectrum.

We first analyze the evolution of the O K-edge spectra with temperature. Since the x-ray transition takes place between the O $1s$ and the O $2p$ levels, no multiplets coming from different final state configurations contribute to the spectra. Thus direct information about the band gap can be obtained by measuring the evolution of the rising edge with temperature. Furthermore, the changes in intensity of the different features in the spectra allow us to understand how hybridization with the Co and La states evolves with temperature.

The intensity at the O K edge in LCO [14,25,27,28] and similar perovskites [32] results from dipolar transitions from the O $1s$ occupied states into the O $2p$ empty states. The latter are hybridized to different orbitals of the other atoms in the compound. Three regions can be differentiated: (i) From 527 to 532 eV, the intensity is ascribed to O $2p$ states hybridized with Co $3d$ states. (ii) Between 532 and 539 eV, the transitions into the hybridized O $2p$–La $5d$ states dominate the signal. (iii) For photon energies above $h\nu > 539$ eV, transitions into the hybridized O $2p$–Co $4sp$ states take place.

The first remarkable feature of the O K-edge XAS spectra as a function of the temperature is the difference in spectral shape between the lowest temperature and the others. At low temperature a narrow peak is observed in the Co $3d$ region that becomes broader and moves to lower photon energies as the temperature increases. This shift, also observed at the rising edge, is indicative of increasing metallization. Between 181 K and room temperature the edge shifts 550 meV to lower photon energies. This shift corresponds to the band gap reduction upon increasing temperature and it is significantly larger than the most recently reported values (≈250 meV) [28]. Furthermore, the La $5d$ region has a threefold structure with a pronounced

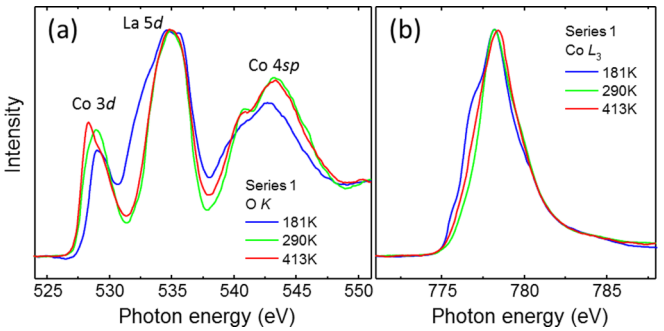

FIG. 3. Temperature evolution of O K-edge (a) and Co L_3-edge (b) XAS spectra, corresponding to the largest populated level at each temperature. The spectra have been normalized to their maxima.

shoulder around 533 eV that disappears upon heating. Finally, the Co 4*sp* region extends to lower photon energies compared to higher temperatures, indicating a narrower bandwidth at 181 K, and the double peak structure is also less pronounced.

The evolution with temperature and in particular the larger value of the gap at low temperature compared to latest reported results [28] suggests that, after the last annealing process or during cooling, adsorption of oxygen at the surface took place resulting in a nonstoichiometric surface termination. Upon heating the sample the excess oxygen would leave the sample between 125 K and room temperature.

Heating above room temperature results in a further reduction of the gap by 115 meV. Since metallization is assumed to be almost completed around the maximum reported temperature (413 K), this is to be expected. Besides the energy shift, the spectral shape also changes in the Co 3*d* region. This time, however, it follows the evolution anticipated across the LS-HS transition [25,27,28]. Thus, a continuous transfer of spectral weight from the pseudo-e_g (≈529 eV) to pseudo-t_{2g} (≈528 eV) region takes place, as expected for increasing HS population with partially unoccupied pseudo-t_{2g} states [Fig. 1(b)].

The XAS scans across the Co L_3 absorption edge displayed in Fig. 3(b) show fewer differences with temperature than those measured at the O *K* edge. The most significant observations are the higher intensity below the white line at 181 K, and the weaker intensity of the shoulder above the white line. These two features can be reconciled with the O *K*-edge spectra by assuming that, due to higher oxygen content at the surface, a compound is formed with a larger band gap and a larger contribution from the HS configuration.

Upon increasing from 181 K to room temperature, the sample initially undergoes a sudden change (as observed at the O *K* edge), after which it stays fairly constant. The changes above room temperature are much weaker than at the O *K* edge. More concretely, a slight shift of the white line to higher photon energies, an increase of the intensity around 777 eV and a small shift to lower binding energies of the leading edge can be observed at 413 K. Together, these observations point towards an increase of the HS population and metallization of the system, in agreement with previous experiments [14,17,27].

The combined analysis of the O *K*-edge and Co L_3-edge data points towards effects with significant influence from the surface stoichiometry. On the one hand, the data at the O *K* edge at 181 K indicate a material less conducting than bulk LCO, suggesting a higher oxidation state. On the other hand, the Co L_3 edge seems to shift to lower photon energies, implying the system is either more metallic or has predominantly HS character. One plausible interpretation of these results is to assume modification of the surface stoichiometry towards $La_{1+x}CoO_{3+x}$, with $x \leqslant 1$. If we assume purely ionic bonding, this would result in the presence of Co^{3-x} ions, which have more HS character and lower conductivity, as observed in La_2CoO_4 [26].

The PEEM images of series 2 as a function of temperature are displayed in Fig. 4 for the O *K* and Co L_3 edges. Improving the spatial resolution by a factor of 5 allows us to observe well resolved features. At 125 K broad dark spots can be observed indicating inhomogeneities similar to those observed in series 1. At 277 K the surface looks much more homogeneous and the broad, dark spots are no longer distinguishable. Upon further heating to 347 K, the measured images stay basically unchanged, except for some very dark spots that become clearer. They are most likely related to surface damage and/or contamination. Little or no correlation among the high intensity domains that should be representative of metallization is observed upon increasing the temperature. This observation does not support a percolation model in which the domains once nucleated are expected to continue increasing. On the contrary they could be ascribed to modification of the surface chemistry, as observed in series 1.

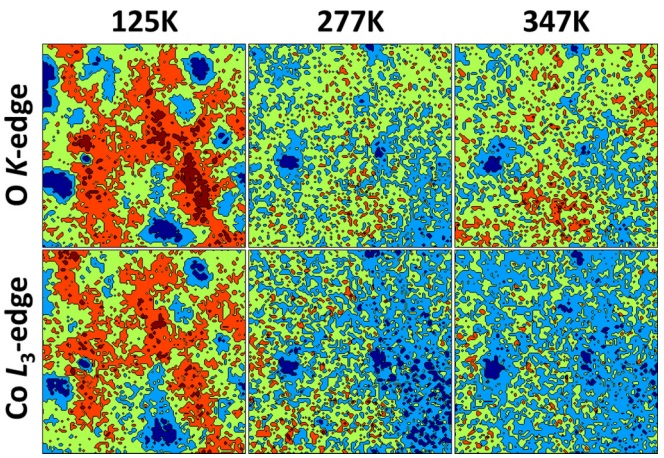

FIG. 4. Temperature evolution of resonant PEEM images (2 × 2 μm^2 fragments) at the O *K* edge, ∼529 eV (top row) and Co L_3 edge, ∼779 eV (bottom row) from the second series of measurements.

The XAS spectra for the oxygen and cobalt edges corresponding to the darkest (level 1) and brightest (level 5) parts of the PEEM images in Fig. 4 are shown in Fig. 5. In Figs. 5(a) and 5(c) the spectra obtained at the O *K* edge are displayed. Figures 5(b) and 5(d) show the Co L_3-edge spectra.

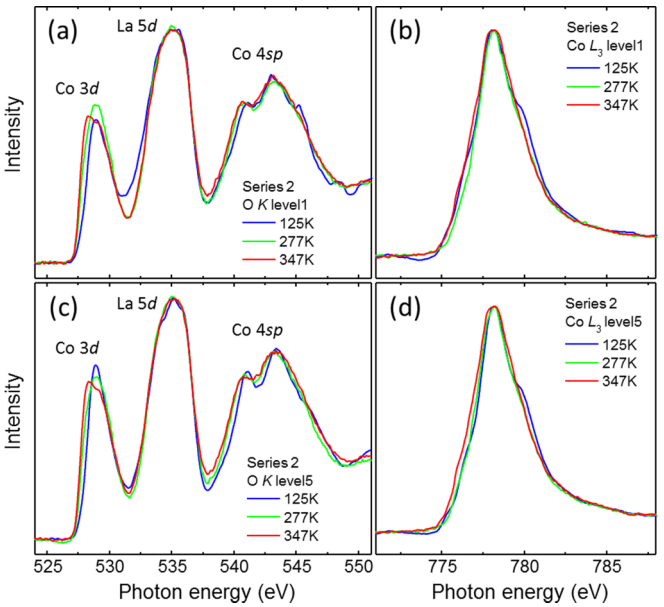

FIG. 5. Temperature evolution of O *K* edge and Co L_3 edge absorption spectra for the darkest (level 1) and the brightest (level 5) areas in the PEEM scans for the second series of measurements.

The data at the O *K* edge show a temperature evolution closer to previous reports [14,28] than that reported for series 1. In particular, between 125 K and room temperature the band gap reduction is 320 and 370 meV for levels 1 and 5, respectively. This value is smaller than that of series 1 and closer to the most recently reported one [28,33]. This confirms that the lowest temperature spectra in series 1 correspond to a nonstoichiometric LCO surface. Between room temperature and the maximum temperature measured (347 K) the gap closes 160 meV for level 1 (dark) and 130 meV for level 5 (bright). Regarding the lineshape, and as described for series 1, the Co 3*d* region experiences the largest changes. It exhibits the redistribution of spectral weight consistent with evolution from a mainly LS configuration with all the pseudo-t_{2g} orbitals filled, to a mixed LS-HS configuration, in which the pseudo-t_{2g} are partially unoccupied [14,27,28]. The comparison between the two levels, 1 and 5, shows that the main differences happen at the lowest temperature. While the temperature evolution for level 5 (bright) is that of stoichiometric LCO, level 1 (dark) at 125 K has some spectral weight between the Co 3*d* and La 5*d* regions. Furthermore, the Co 4*sp* region has now a lineshape similar to that expected for stoichiometric LCO.

The results for the Co L_3 edge follow the trend observed at the O *K* edge. Fewer changes with temperature are observed than in series 1, especially when comparing low temperature and room temperature data. Nevertheless, a decrease of the intensity at the high-energy shoulder of the white line is observed, as expected for a reduction of the LS population. The spectra at level 1 and level 5 exhibit qualitatively similar behavior with temperature. The sample seems to be more stoichiometric with a larger HS contribution, as discussed for the O *K* edge.

The analysis of the XAS spectra from series 2 shows changes with temperature in all spatial areas of the surface expected for stoichiometric LCO. At the O *K* edge we see upon heating a shift of the absorption edge to lower energies, corresponding to metallization of the compound. At the Co L_3 edge we see changes of the spectral shape consistent with the LS-HS transition. The HS state content develops upon increasing temperature. However, at low temperature the surface stoichiometry deviates still from that of LCO, as for the first series. Since the annealing was done in an oxygen atmosphere, and after annealing no carbon contamination was observed, the most plausible explanation of the observed phenomena is that we start with an oxygen-rich surface with a larger band gap than in stoichiometric LCO. The formation of a $La_{1+x}CoO_{3+x}$ phase at the surface is a very natural explanation since, due to the presence of Co^{2+}, as is the case for La_2CoO_4 [26], the surface has lower conductivity and a higher HS population than stoichiometric LCO. During the first heating cycle, oxygen desorbs from the surface, bringing the stoichiometry closer to LCO. As a consequence, the second series shows a behavior similar to that expected for the stoichiometric compound. However, the dark regions in the PEEM scans still reveal slightly different stoichiometry, as confirmed by the changes in the lineshape of the XAS spectra.

Besides the stoichiometry, we would like to emphasize that the same transfer of intensity from the high energy (LS) state to the low energy (HS or Co^{2+}) state shoulder in Co L_3-edge absorption spectra is observed both upon heating and when going from the bright to the dark areas of the PEEM image. This suggests that the Co spin state varies not only with the temperature, but also depends on the structural and chemical properties of each particular surface region. Therefore, the present study shows that besides strain, the electronic properties at the surface can be modified by the preparation procedure. These effects could be further enhanced by using stepped surfaces.

The continuous semiconductor-to-metal transition resulting from our experiments goes along with the current understanding of the system. From the experimental side, the presence of well defined nanometer size metallic domains with a HS configuration would result in the development of magnetic ordering not observed in bulk $LaCoO_3$. From the theoretical side, charge disproportionation and spin fluctuations have been shown to take place within a single unit cell when doing calculations within the dynamical mean-field theory (DMFT) formalism required to properly treat the system due to its paramagnetic nature [20,21,29]. This supports a microscopic evolution of the spin and charge state of the system. At room temperature the LS-HS population has been proposed to have a 50%-50% occupation [20]. This means that we should have a homogeneous state already at room temperature and from there on the metallic transition will proceed also in a continuous manner. In this respect, trying to follow the local evolution of the spin system with atomically resolved probes such as scanning tunneling microscopy or high resolution electron microscopy will be an interesting continuation of this work. Indeed the later technique has shown the presence of atomically ordered spin states induced by the substrate strain in $LaCoO_3$ thin films [23,34].

IV. CONCLUSIONS

We have studied the spatial modifications of the electronic structure of LCO with temperature. The results show inhomogeneities in the PEEM images and XAS spectra only at low temperatures, just above the spin transition. They are related to deviations from the LCO stoichiometry at the surface due to inhomogeneous oxidation during sample preparation. At room temperature and above, a smooth evolution with temperature is observed in both the images and in the corresponding spectra. No correlation between the high intensity regions ascribed to the metallic domain with temperature is observed. This suggests that metallization does not take place by percolation of domains, as proposed by Goodenough in the early 1970s [10,11]. The presented results support the current theoretical understanding of $LaCoO_3$ which allows one to have charge disproportionation and different spin states within a unit cell, which would favor then a microscopic explanation for the semiconductor to metal transition. The fact that similar changes in the electronic properties with temperature can be realized by modifying the surface stoichiometry opens a new route to design interfaces with controlled catalytic activity for the selected applications.

ACKNOWLEDGMENT

This project was supported by the BMBF proposal 05K12GU2. M.E.D. acknowledges support from the Projects No. AYA2012-39832-C02-01/02 and ESP2015-67842-P of MINECO of Spain.

[1] N. B. Ivanova, S. G. Ovchinnikov, M. M. Korshunov, I. M. Eremin, and N. V. Kazak, Phys. Usp. **52**, 789 (2009).
[2] N. Li, A. Boréave, J.-P. Deloume, and F. Gaillard, Solid State Ionics **179**, 1396 (2008).
[3] M. Alifanti, J. Kirchnerova, B. Delmon, and D. Klvana, Appl. Catal. A **262**, 167 (2004).
[4] M. C. Álvarez-Galván, D. A. Constantinou, R. M. Navarro, J. A. Villoria, J. L. G. Fierro, and A. M. Efstathiou, Appl. Catal. B **102**, 291 (2011).
[5] C. H. Kim, G. Qi, K. Dahlberg, and W. Li, Science **327**, 1624 (2010).
[6] F. Rivadulla, Z. Bi, E. Bauer, B. Rivas-Murias, J. M. Vila-Fungueiriño, and Q. Jia, Chem. Mater. **25**, 55 (2013).
[7] M. Kubicek, Z. Cai, W. Ma, B. Yildiz, H. Hutter, and J. Fleig, ACS Nano **7**, 3276 (2013).
[8] P. G. Radaelli and S.-W. Cheong, Phys. Rev. B **66**, 094408 (2002).
[9] S. Yamaguchi, Y. Okimoto, and Y. Tokura, Phys. Rev. B **55**, R8666 (1997).
[10] P. M. Raccah and J. B. Goodenough, Phys. Rev. **155**, 932 (1967).
[11] M. A. Señariz-Rodríguez and J. B. Goodenough, J. Solid State Chem. **116**, 224 (1995).
[12] Y. Kobayashi, T. S. Naing, M. Suzuki, M. Akimitsu, K. Asai, K. Yamada, J. Akimitsu, P. Manuel, J. M. Tranquada, and G. Shirane, Phys. Rev. B **72**, 174405 (2005).
[13] N. Orlovskaya, D. Steinmetz, S.Yarmolenko, D. Pai, J. Sankar, and J. Goodenough, Phys. Rev. B **72**, 014122 (2005).
[14] M. Abbate, J. C. Fuggle, A. Fujimori, L. H. Tjeng, C. T. Chen, R. Potze, G. A. Sawatzky, H. Eisaki, and S. Uchida, Phys. Rev. B **47**, 16124 (1993).
[15] M. A. Korotin, S. Y. Ezhov, I. V. Solovyev, V. I. Anisimov, D. I. Khomskii, and G. A. Sawatzky, Phys. Rev. B **54**, 5309 (1996).
[16] Z. Ropka and R. Radwanski, Physica B: Condens. Matter **312-313**, 777 (2002).
[17] M. W. Haverkort, Z. Hu, J. C. Cezar, T. Burnus, H. Hartmann, M. Reuther, C. Zobel, T. Lorenz, A. Tanaka, N. B. Brookes, H. H. Hsieh, H.-J. Lin, C. T. Chen, and L. H. Tjeng, Phys. Rev. Lett. **97**, 176405 (2006).
[18] K. Knížek, Z. Jirák, J. Hejtmánek, and P. Novák, J. Phys.: Condens. Matter **18**, 3285 (2006).
[19] K. Knížek, Z. Jirák, J. Hejtmánek, P. Novák, and W. Ku, Phys. Rev. B **79**, 014430 (2009).
[20] V. Křápek, P. Novák, J. Kuneš, D. Novoselov, D. M. Korotin, and V. I. Anisimov, Phys. Rev. B **86**, 195104 (2012).
[21] M. Karolak, M. Izquierdo, S. L. Molodtsov, and A. I. Lichtenstein, Phys. Rev. Lett. **115**, 046401 (2015).
[22] S. N. Vereshchagin, L. A. Solovyov, E. V. Rabchevskii, V. A. Dudnikov, S. G. Ovchinnikov, and A. G. Anshits, Chem. Commun. **50**, 6112 (2014).
[23] W. S. Choi, J.-H. Kwon, H. Jeen, J. E. Hamann-Borrero, A. Radi, S. Macke, R. Sutarto, F. He, G. A. Sawatzky, V. Hinkov, M. Kim, and H. N. Lee, Nano Lett. **12**, 4966 (2012).
[24] L. Richter, S. D. Bader, and M. B. Brodsky, Phys. Rev. B **22**, 3059 (1980).
[25] F. M. F. de Groot, M. Abbate, J. van Elp, G. A. Sawatzky, Y. J. Ma, C. T. Chen, and F. Sette, J. Phys.: Condens. Matter **5**, 2277 (1993).
[26] M. Merz, D. Fuchs, A. Assmann, S. Uebe, H. v. Löhneysen, P. Nagel, and S. Schuppler, Phys. Rev. B **84**, 014436 (2011).
[27] M. Izquierdo, M. Karolak, C. Trabant, K. Holldack, A. Föhlisch, K. Kummer, D. Prabhakaran, A. T. Boothroyd, M. Spiwek, A. Belozerov, A. Poteryaev, A. Lichtenstein, and S. L. Molodtsov, Phys. Rev. B **90**, 235128 (2014).
[28] Z. Hu, H. Wu, T. C. Koethe, S. N. Barilo, S. V. Shiryaev, G. L. Bychkov, C. Schüssler-Langeheine, T. Lorenz, A. Tanaka, H. H. Hsieh, H.-J. Lin, C. T. Chen, N. B. Brookes, S. Agrestini, Y.-Y. Chin, M. Rotter, and L. H. Tjeng, New J. Phys. **14**, 123025 (2012).
[29] K. Kuneš and V. Křápek, Phys. Rev. Lett. **106**, 256401 (2011).
[30] M. S. D. Read, M. S. Islam, G. W. Watson, F. King, and F. E. Hancock, J. Mater. Chem. **10**, 2298 (2000).
[31] S. Khan, R. J. Oldman, F. Cora, C. R. A. Catlow, S. A. French, and S. A. Axon, Phys. Chem. Chem. Phys. **8**, 5207 (2006).
[32] J. Suntivich, W. T. Hong, Y.-L. Lee, J. M. Rondinelli, W. Yang, J. B. Goodenough, B. Dabrowski, J. W. Freeland, and Y. Shao-Horn, J. Phys. Chem. C **118**, 1856 (2014).
[33] A. Doi, J. Fujioka, T. Fukuda, S. Tsutsui, D. Okuyama, Y. Taguchi, T. Arima, A. Q. R. Baron, and Y. Tokura, Phys. Rev. B **90**, 081109(R) (2014).
[34] J.-H. Kwon, W. S. Choi, Y.-K. Kwon, R. Jung, J.-M. Zuo, H. N. Lee, and M. Kim, Chem. Mater. **26**, 2496 (2014).